**Biogeosciences
Discussions**

Overlooked runaway feedback in the marine nitrogen cycle: the vicious cycle

A. Landolfi, H. Dietze, W. Koeve, and A. Oschlies

GEOMAR Helmholtz-Zentrum für Ozeanforschung Kiel, Marine Biogeochemical Modelling, Düsternbrooker Weg 20, 24105 Kiel, Germany

Correspondence to: A. Landolfi (alandolfi@geomar.de)

BGD

9, 8905–8930, 2012

The vicious N cycle

A. Landolfi

Title Page

Abstract	Introduction
Conclusions	References
Tables	Figures

|◄ | ►|

◄ | ►

Back | Close

Full Screen / Esc

Printer-friendly Version

Interactive Discussion

Abstract

The marine nitrogen (N) inventory is controlled by the interplay of nitrogen loss processes, here referred to as denitrification, and nitrogen source processes, primarily nitrogen fixation. The apparent stability of the marine N inventory on time scales longer than the estimated N residence time, suggests some intimate balance between N sinks and sources. Such a balance may be perceived easier to achieve when N sinks and sources occur in close spatial proximity, and some studies have interpreted observational evidence for such a proximity as indication for a stabilizing feedback processes. Using a biogeochemical ocean circulation model, we here show instead that a close spatial association of N_2 fixation and denitrification can, in fact, trigger destabilizing feedbacks on the N inventory and, because of stoichiometric constrains, lead to net N losses. Contrary to current notion, a balanced N inventory requires a regional separation of N sources and sinks. This can be brought about by factors that reduce the growth of diazotrophs, such as iron, or by factors that affect the fate of the fixed nitrogen remineralization, such as dissolved organic matter dynamics. In light of our findings we suggest that spatial arrangements of N sinks and sources have to be accounted for in addition to individual rate estimates for reconstructing past, evaluating present and predicting future marine N inventory imbalances.

1 Introduction

Variations in the oceanic fixed-nitrogen (N) inventory are known to have driven marine productivity changes contributing to atmospheric CO_2 variations in Earth's history (Falkowski, 1997; Altabet et al., 2002). For the last several thousand years, however, the apparent stability of the N inventory over several oceanic N residence time-scales (Gruber, 2004; Altabet, 2007) suggests an approximate balance of the main N source, the diazotrophic fixation of N_2 gas, and the main N loss process associated with organic matter remineralization under low oxygen concentrations, referred to as denitrification

(Devol et al., 2008). The N inventory is thought to be stabilized by feedback mechanisms (Codispoti, 1989) that limit and reduce the strong excursions of the marine N content with respect to the more slowly overturning P inventory (Delaney, 1998). The current paradigm assumes that slowly-growing N_2 fixers (Capone et al., 1997) have
5   a competitive advantage over non-fixing phytoplankton in waters where N is in deficit relative to phosphate (Redfield et al., 1963; Tyrrel, 1999). As a "side effect" of adding N without any equivalent P, diazotrophs tend to reduce their own niche (Fig. 1a) (Tyrrel, 1999). Similarly, denitrification limits itself by reducing the amount of fixed nitrogen eventually upwelling into the light-lit layer, and thereby reducing the growth of "ordi-
10 nary" phytoplankton, subsequent export of organic matter, oxygen consumption and, eventually, denitrification at depth (Fig. 1b) (Codispoti, 1989). Individually, both nitrogen fixation and denitrification initiate negative feedbacks that limit N inventory excursions and act as self-limiting processes (Codispoti, 1989; Gruber, 2004) (Fig. 1a, b). With their mutual interactions these antagonistic processes work against the development
15 of substantial N deficits or surpluses relative to P (Codispoti, 1989; Tyrrel, 1999; Gruber, 2004). According to this picture, any N deficit resulting from denitrification also gives rise to an excess of phosphate relative to nitrate which tends to stimulate the growth of N_2 fixers (Fig. 1a) (Redfield et al., 1963; Tyrrel, 1999). N addition via N_2 fixation enhances the export of organic matter and oxygen consumption at depth which,
20 in turn, will enhance the loss of fixed N via denitrification (Fig. 1b) (Codispoti, 1989).

Traditionally the two processes were considered to be spatially disconnected in the current ocean, because of factors such as iron limitation (Moore et al., 2009), temperature limits (Breitbarth et al., 2007) and macro-nutrient effects (Mills and Arrigo, 2010), that reduce the diazotrophs' ability to respond locally to N deficits (Redfield et al., 1963;
25 Codispoti, 1989; Falkowski, 1997; Tyrrel, 1999; Lenton and Watson, 2000; Moore and Doney, 2007; Mills and Arrigo, 2010). The wider the spatial separation, the longer the response time and the larger the potential for changes in the marine N inventory. This view of a remote connection between these two counteracting processes has been difficult to reconcile with the apparent stability of the marine N inventory (Gruber, 2004;

Altabet, 2007). Recent observational inferences of a close spatial proximity of N_2 fixers and denitrification in the eastern South Pacific have thus been interpreted as a welcome indication of a fast and stabilizing feedback mechanism (Deutsch et al., 2007; Fernandez et al., 2011) promoting a balanced N inventory (Gruber, 2004).

Here we investigate the implications of a tight spatial coupling of denitrification and N_2 fixation in a state-of-the-art coupled biogeochemical (Schmittner et al., 2008) circulation model (Gnanadesikan et al., 2005). A number of sensitivity experiments examine how different parameterizations of the marine N cycle, specifically designed to differ in the mutual interaction of nitrogen fixation and denitrification, allow the model to maintain the marine N inventory. We asses the implications of our finding on the current understanding of the marine N inventory controls.

2 Methods

The coupled ocean-ice model used here correspond to the CM2.1 (Gnanadesikan et al., 2005) configuration with a $3° \times 2°$ resolution and 28 vertical levels. The model was forced by monthly heat and freshwater fluxes and wind fields taken from the climatological dataset of the Coordinated Ocean Reference Experiments (CORE) which is based on the work of Large and Yeager (2004). The circulation model is initialized with annual mean temperature and salinity from the World Ocean Atlas 2001 (Conkright et al., 2002). After a 20 yr integration the circulation model is coupled online to a modified version of the NPZD-type ecosystem model of Schmittner et al. (2008) initialized with observed nutrient and oxygen distributions (Conkright et al., 2002). The ecosystem model has 10 prognostic variables: dissolved oxygen, nitrate, phosphate, (nonnitrogen-fixing) "ordinary" phytoplankton, nitrogen-fixing phytoplankton (diazotrophs), zooplankton and particulate phosphorus and nitrogen detritus and, in sensitivity experiment DOM, semi-labile dissolved organic phosphorus and nitrogen. Diazotrophs are modeled explicitly, with a growth rate lower than that of "ordinary" phytoplankton. Diazotrophs can take up nitrate but are only limited by phosphate. Wherever simulated

The vicious N cycle

A. Landolfi

oxygen concentrations fall below 5 mmol m^{-3}, nitrate is used as electron acceptor to remineralize organic matter through the process of denitrification (Devol et al., 2008). In this study, sedimentary denitrification is not considered as we do not resolve shelf and costal seas. A detailed model description is given in the Appendix. The simulations we performed are: (1) CONTROL is the control simulation where the ecosystem parameters follow the elemental stoichiometry of Anderson (1995). (2) NOFIX is the same as the control simulation but with N$_2$ fixation switched off. (3) IRON is as the control simulation with the addition of a formulation mimicking iron stress on diazotrophs and non-fixing phytoplankton. Specifically, phytoplankton and diazotroph growth rates are reduced by a factor of 0.5 and 0.8, respectively when modeled surface PO$_4$ concentrations are lower than observed monthly mean PO$_4$ values taken from the World Ocean Atlas (WOA) (Conkright et al., 2002) (Fig. A1). Without an explicit representation of iron, this is to mimic the effects of iron limitation in regions where WOA surface inorganic nutrients are not completely drawn down such as, the high nutrient low chlorophyll (HNLC) regions. (4) DOM is a simulation that, in addition to the iron limitation formulation, includes DON and DOP compartments and allows diazotrophs to use DOP as a P source when PO$_4$ concentrations are lower than 5 µmol P m^{-3}. All model runs are integrated for 150 yr. This relatively short integration period limits the drift from observed nutrient and oxygen concentrations.

3   Results and discussion

All simulations display high biological production in the upwelling regions of the equatorial Eastern Pacific, the Indian Ocean and the Benguela upwelling system. These regions are associated with high export, subsequent remineralization and oxygen consumption at depth, contributing to maintain the oxygen minimum zones (OMZs) in the Pacific and Indian Ocean. In our CONTROL model configuration, denitrification and N$_2$ fixation are free to interact. N-deficient waters provide an ecological niche for the simulated diazotrophs. Iron limitation is not accounted for in the CONTROL configuration,
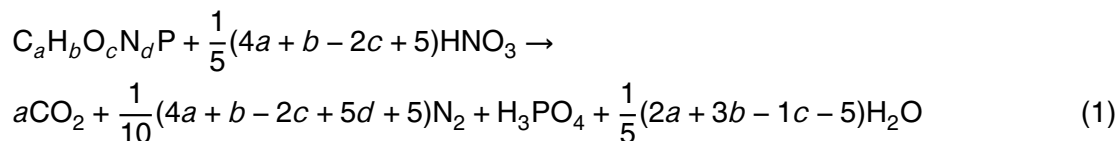
Full Screen / Esc

Printer-friendly Version

Interactive Discussion

where surface temperatures above 15 °C and N-deficiency are the essential controls on the growth of diazotrophs. Thereby, simulated N_2 fixation can quickly respond to the N-deficit of denitrified waters upwelled from low-oxygen regions of the temperate ocean. Areas of simulated N_2 fixation are located mainly along the eastern boundaries of the tropical ocean (Fig. 2a), in close agreement with recent inferences based on observed biogeochemical tracer distributions (Deutsch et al., 2007). Despite the fast response of N_2 fixation to the N deficit generated by denitrification, the total N inventory rapidly decreases in the CONTROL run by about 6.4 % within 150 yr (Fig. 3a). In fact, simulated denitrification rates exceed N_2 fixation rates by more than a factor 4 within a few years after having initialized the model with observed tracer distributions (Fig. 3c). A systematic loss of fixed nitrogen has also been found in earlier modeling studies (Moore and Doney, 2007; Schmittner et al., 2008) and will here be explained by a positive and previously overlooked feedback: the extra production and export of organic matter associated with newly fixed nitrogen enhances denitrification (Fig. 3b) which, in turn, enhances the nitrate deficit and favors further N_2 fixation above the OMZ (Fig. 1c). Because of stoichiometric constraints, this positive feedback leads to a vicious cycle with a net loss of fixed nitrogen. Organic matter that undergoes complete denitrification (implicitly including the anammox reaction) follows the stoichiometry (Paulmier et al., 2009):

$$C_aH_bO_cN_dP + \frac{1}{5}(4a + b - 2c + 5)HNO_3 \rightarrow$$

$$aCO_2 + \frac{1}{10}(4a + b - 2c + 5d + 5)N_2 + H_3PO_4 + \frac{1}{5}(2a + 3b - 1c - 5)H_2O \qquad (1)$$

where a, b, c, d are the assumed stoichiometric ratios of organic matter $C_a : H_b : O_c : N_d : P$. It follows that for each mole of organic nitrogen denitrified, $R_{N_{loss}} = \frac{1}{5d}(4a + b - 2c + 5d + 5)$ moles of nitrate are lost (Paulmier et al., 2009). For typical organic matter with a stoichiometry of $C_{106} : H_{175} : O_{42} : N_{16} : P$ (Anderson, 1995) $R_{N_{loss}} = 7.5$ moles of nitrogen are lost for every mole of organic nitrogen denitrified. This implies that in

regions where suboxic remineralization is larger than about 1/7th of the vertically integrated remineralization a vicious cycle will ensue. Different stoichiometries of OM falling into the OMZ may modulate the magnitude of the N loss: Denitrification of organic matter with increased carbon content, relative to $C_{106} : H_{175} : O_{42} : N_{16} : P$, results in increased N losses. Denitrification of organic matter with lower C : N, e.g. algal proteins ($C_5 3 : H_7 : O_{23} : N_{16}$) (Laws, 1991), would, on the other hand reduce the $R_{N_{loss}}$ to values as low as 2.2. Plausible stoichiometries of marine organic matter (Laws, 1991), all yield $R_{N_{loss}} > 1$ and, denitrification of organic matter derived from N_2-fixation will always lead to a net loss of fixed nitrogen. Once upwelled to the surface, denitrified waters further stimulate nitrogen fixation closing the vicious cycle (Fig. 1c). In our CONTROL run, where on average approximately 60 % of the simulated N_2 fixation occurs above suboxic waters (Fig. 2a), this vicious cycle leads to more N being denitrified than fixed (Fig. 3d) and a declining total N inventory (Fig. 3a). This result is qualitatively consistent with that of an earlier idealized box model (Canfield, 2006) of a costal upwelling setting that included a parameterization of sedimentary denitrification.

A second simulation NOFIX, which differs from the CONTROL run only in that N_2 fixation is turned off, provides an estimate of the potential strength of the vicious cycle. As expected, without nitrogen fixation but with denitrification turned on, the model cannot maintain its nitrogen inventory and loses about 4.6 % of the fixed N within 150 yr (Fig. 3a). This loss is, however, smaller than the net nitrogen loss simulated by the CONTROL experiment (6.4 %, Fig. 3a) where the N_2 fixation sustains the vicious cycle. After 150 yr, the total N loss of the CONTROL simulation is about 40 % larger than in experiment NOFIX.

We now test, with additional simulations, how a spatial separation of N_2 fixation and denitrification affects the modeled N inventory. In experiment IRON, growth rates of both diazotrophs and ordinary phytoplankton are reduced in regions where simulated surface PO_4 concentrations fall below observed monthly mean PO_4 values taken from the World Ocean Atlas (Conkright et al., 2002), mimicking the effect of iron limitation in our model that does not explicitly resolve the micronutrient iron. When simulating iron

The vicious N cycle

A. Landolfi

limitation, the upwelled excess phosphate is not immediately available to diazotrophs above the OMZ. The growth of N_2 fixers in experiment IRON is thus shifted westwards relative to the CONTROL run, thereby contributing to a separation of N_2 fixation and denitrification (Fig. 2c). In the 150-yr average, 35 % of the simulated N_2 fixation occurs above OMZs in experiment IRON as compared to 60 % in the CONTROL run. The reduced export and subsequent remineralization of organic material in the OMZ region leads to a reduction of the modeled oxygen demand and the associated low-oxygen zone (Fig. 4b). The partial shift of areas of N_2 fixation away from those of denitrification in experiment IRON reduces the fraction of export production that is remineralized in OMZ's relative to the CONTROL simulation (Fig. 5a, c) resulting in a smaller (5 %) decline of the fixed N inventory within 150 yr (Fig. 3a, c, d).

A model configuration able to maintain the observed marine nitrogen inventory (Fig. 3a, d) is obtained by including, in addition to iron limitation, a dissolved organic nitrogen (DON) and phosphorus (DOP) pool in experiment DOM. In this simulation, a portion of organic matter is channeled into DON and DOP (Fig. 6), which can be advected away from their source regions and thereby allow for a lateral separation of nutrient fluxes into the surface layer from export of organic matter back into the ocean interior (Fig. 1d). Further in this simulation, DOP is an additional phosphorus source to diazotrophs at very low phosphate concentrations. The DOM configuration permits the transport of the upwelled excess phosphorous signal into areas laterally disconnected from the OMZ allowing for a wider spatial separation of N_2 fixation and denitrification (Fig. 2d). During the 150-yr simulation, only 20 % of the simulated N_2 fixation takes place above suboxic waters, as opposed to 35 % and 60 % in the IRON and CON-TROL simulations, respectively. This spatial separation of diazotrophic activity from denitrification combined with the vertical separation of dissolved organic matter aerobic remineralization from the deeper depth horizon of the OMZ leads to a drastic reduction of the region where the vicious cycle takes place (Fig. 5), which, in turn, decreases denitrification rates relative to those of N_2 fixation (Fig. 3c, d). On the 150-yr timescale

The vicious N cycle

A. Landolfi

Title Page

Abstract	Introduction
Conclusions	References
Tables	Figures

◄◄　　►►

◄　　►

Back　　Close

Full Screen / Esc

Printer-friendly Version

Interactive Discussion

considered in our simulations, the marine N budget of the DOM model configuration is essentially balanced (Fig. 3a).

4 Conclusions

The positive feedbacks between denitrification and N_2 fixation emerging from the spatial proximity of denitrification and N_2 fixation sites give rise to a vicious cycle where positive feedbacks persist: decreased N availability occurs proximate to denitrifying areas where excess phosphate stimulates N_2 fixation activity (positive feedback). This in turn enhances organic matter export and oxygen consumption at depth fueling denitrification further (positive feedback). Because of stoichiometric constraints, any enhancement of N_2 fixation results in a net loss of marine nitrogen if a substantial portion of the newly fixed organic N is remineralized with NO_3 as the ultimate electron acceptor. Factors controlling the growth of diazotrophs, such as iron limitation and temperature, and factors that control the fate of the fixed nitrogen, such as DOM dynamics and oxygen distributions and transport, allow to disconnect the flux of newly fixed organic nitrogen into the low-oxygen areas of denitrification. Accounting for these controls is critical for breaking the vicious cycle that, otherwise, can be found to lead to a complete regional loss of fixed nitrogen in biogeochemical ocean models (Moore and Doney, 2007; Schmittner et al., 2008). A complete loss of fixed nitrogen is rarely observed in the open ocean, suggesting that the vicious cycle is efficiently suppressed in reality (Fig. 5d). Iron and temperature limitation of diazotrophs growth, DOM dynamics, but also lateral injections of O_2 into oxygen minimum zone not captured by our model, are all likely contributing to the suppression of the modern ocean vicious cycle.

Challenging the current understanding of the marine N inventory controls, we demonstrate that spatial distance rather than spatial proximity promotes negative feedbacks that stabilize the marine nitrogen inventory. If the vicious cycle is taken into account, the two apparently opposite views of balance of the modern N inventory (Codispoti et al., 2001; Deutsch et al., 2007) converge. Our results have important implications

for understanding the controls on the marine global N inventory and predicting its response to climate change. We suggest that large changes in the marine N inventory can be triggered by changes in the spatial arrangement of N_2 fixation and N loss regions and do not need to be initiated by a change in rates of either process. Sources of new nitrogen, via N_2 fixation (Deutsch et al., 2007; Fernandez et al., 2011) and atmospheric deposition (Duce et al., 2008), can lead to a net N loss (Codispoti et al., 2001) rather than a net gain once located within or above oxygen minimum zones. The likely future expansion of diazotrophs' temperature-optima domain (Breitbarth et al., 2007; Moisander et al., 2008), the ongoing expansion of OMZs (Stramma et al., 2008) and the climate-driven changes in dust deposition patterns (Mahowald et al., 2008), all suggest a more intimate spatial coupling of N_2 fixation activity to denitrification over the next decades, which may lead to a net loss of marine nitrogen (Codispoti et al., 2001) with consequent impacts on ocean productivity and marine CO_2 uptake (Falkowski, 1997). We suggest that any quantitative assessment of past and expected future changes in the marine N inventory (Codispoti et al., 2001) cannot rely solely on individual estimates of N loss and N gain processes, but has to account for their spatial relationship.

Appendix A

A1   Ecosystem model equations

Each prognostic variable C is determined following:

$$\frac{\partial C}{\partial t} = T + \text{sms}, \tag{A1}$$

where T represents all diffusive and advective transport terms. sms denote the source minus sink terms, which describe the biogeochemical interactions as follows:

Nitrate (NO_3) equation:

$$\text{sms}(NO_3) = -\bar{J}P - u_N\overline{J_{Dia}}P_{Dia} + (\mu_{D_N}(1 - \sigma_{D_N})D_N + \gamma_2(1 - \sigma_{Z_e})Z + \mu_{DON}DON)$$
$$(1 - 0.8R_O R^{-1} r_{sox}^{NO_3}) \tag{A2}$$

Phosphate (PO_4) equation:

$$\text{sms}(PO_4) = (+\gamma_2(1 - \sigma_{Z_e})Z - \bar{J}P)R^{-1} - \overline{J_{Dia}}P_{Dia}R_{Dia}^{-1} + \mu_{D_P}(1 - \sigma_{D_P})D_P + \mu_{DOP}DOP \tag{A3}$$

Phytoplankton (P) equation:

$$\text{sms}(P) = \bar{J}P - G(P)Z - \mu_P P \tag{A4}$$

Diazotroph (P_{Dia}) equation:

$$\text{sms}(P_{Dia}) = \overline{J_{Dia}}P_{Dia} + \overline{J_{Dia_{DOP}}}P_{Dia} - G(P_{Dia})Z - \mu_{PDia}P_{Dia} \tag{A5}$$

Zooplankton (Z) equation:

$$\text{sms}(Z) = \gamma_1(G(P)Z + G(P_{Dia})Z) - \gamma_2 Z - \mu_Z Z^2 \tag{A6}$$

Nitrogen detritus (D_N) equation:

$$\text{sms}(D_N) = (1 - \gamma_1)(1 - \sigma_{Z_s})(G(P) + G(P_{Dia}))Z + \mu_P(1 - \sigma_{P_m})P + \mu_{P_{Dia}}(1 - \sigma_{Dia_m})P_{Dia}$$
$$+ \mu_Z(1 - \sigma_{Z_m})Z^2 - \mu_{D_N}D_N - w_s\frac{\partial D_N}{\partial z} \tag{A7}$$

Phosphorus detritus (D_P) equation:

$$\text{sms}(D_P) = ((1 - \gamma_1)(1 - \sigma_{Z_s})(G(P) + G(P_{Dia}))Z + \mu_P(1 - \sigma_{P_m})P + \mu_Z(1 - \sigma_{Z_m})Z^2)R^{-1}$$
$$+ \mu_{P_{Dia}}(1 - \sigma_{Dia_m})P_{Dia}R_{Dia}^{-1} - \mu_{D_P}D_P - w_s\frac{\partial D_P}{\partial z} \tag{A8}$$

Oxygen (O_2) equation:

$$\text{sms}(O_2) = F_{\text{sfc}}(\overline{J}P + \overline{J_{\text{Dia}}}P_{\text{Dia}}(\mu_{D_N}(1 - \sigma_{D_N})D_N + \mu_{\text{DON}}\text{DON}$$
$$+ \gamma_2(1 - \sigma_{Z_e})Z)r_{\text{sox}}{}^{O_2})R^{-1}R_O \tag{A9}$$

Dissolved organic nitrogen equation (DON)

$$\text{sms}(\text{DON}) = \sigma_{Z_s}(1 - \gamma_1)(G(P) + G(P_{\text{Dia}}))Z + \sigma_{P_m}\mu_P P + \sigma_{Z_m}\mu_Z Z^2 + \sigma_{Z_e}\gamma_2 Z$$
$$+ \sigma_{\text{Dia}_m}\mu_{P_{\text{Dia}}}P_{\text{Dia}} + \sigma_{D_N}\mu_{D_N}D_N - \mu_{\text{DON}}\text{DON} \tag{A10}$$

Dissolved organic phosphorus equation (DOP)

$$\text{sms}(\text{DOP}) = (\sigma_{Z_s}(1 - \gamma_1)(G(P) + G(P_{\text{Dia}}))Z + \sigma_{P_m}\mu_P P + \sigma_{Z_m}\mu_Z Z^2 + \sigma_{Z_e}\gamma_2 Z)R^{-1}$$
$$+ \sigma_{\text{Dia}_m}\mu_{P_{\text{Dia}}}P_{\text{Dia}}R_{\text{Dia}}{}^{-1} + \sigma_{D_P}\mu_{D_P}D_P - \mu_{\text{DOP}}\text{DOP} - \overline{J_{\text{Dia}_{\text{DOP}}}}P_{\text{Dia}}R_{\text{Dia}}{}^{-1} \tag{A11}$$

Sources of dissolved organic nitrogen and phosphorus are (1) Fraction of zooplankton sloppy-feeding (2) Fraction of zooplankton excretion (3) Fraction of detritus dissolution (4) Fraction of phytoplankton, diazotrophos and zooplankton mortality. The latter term mimics the mortality by viral infection and phytoplankton cell leakage, however it is not meant to represent phytoplankton passive exudation as this term is expected to be dominated by carbohydrates. Sinks of DON and DOP are through remineralization, which can be different from one another. Uptake of DOP by diazotrophs can occur when phosphate is lower than $0.005\,\text{mmol}\,\text{m}^{-3}$.

A2 Phytoplankton and diazotroph growth

The function $\overline{J} = \overline{J}(I, NO_3, PO_4)$ provides the growth rate of non-diazotrophic phytoplankton determined from irradiance $(I), NO_3, PO_4$,

$$\overline{J}(I, NO_3, PO_4) = \min(J_I, J_{\text{max}}u_{NO_3}, J_{\text{max}}u_{PO_4}), \tag{A12}$$

The maximum growth rate J_{max} is a function of temperature (T):

$$J_{max}(T) = a \cdot \exp\left(\frac{T}{T_b}\right) \qquad (A13)$$

such that growth rates increase by a factor of ten over the temperature range of -2 to $34\,^{\circ}$C. We use $a = 0.6\,\mathrm{d}^{-1}$ for the maximum growth rate at $0\,^{\circ}$C. Under nutrient-replete conditions, the light-limited growth rate J_l is calculated according to:

$$J_l = \frac{J_{max}\alpha I}{\left[J_{max}^2 + (\alpha I)^2\right]^{1/2}} \qquad (A14)$$

where α is the initial slope of the photosynthesis vs. irradiance (P–I) curve. The calculation of the photosynthetically active shortwave radiation I and the method of averaging the light-limited growth over one day is described in Schmittner et al. (2008). Nutrient limitation is represented by the product of J_{max} and the nutrient uptake rates $u_{NO_3} = NO_3/(k_{NO_3} + NO_3)$ and $u_{PO_4} = PO_4/(k_{PO_4} + PO_4)$, with $k_{PO_4} = k_{NO_3} R_{PO_4:NO_3}$ providing the respective nutrient uptake rates. Diazotrophs grow according to the same principles as the other phytoplankton, i.e. their light-limited growth rate $J_{l\,Dia}$ follows

$$J_{l\,Dia} = \frac{J_{max\,Dia}\alpha I}{\left[J_{max\,Dia}^2 + (\alpha I)^2\right]^{1/2}}, \qquad (A15)$$

but are disadvantaged by a lower maximum growth rate, $J_{max\,Dia}$, which is zero below $15\,^{\circ}$C :

$$J_{max\,Dia} = c_{Dia} \max\left(0, a\left(\exp\left(\frac{T}{T_b}\right) - 2.61\right)\right) \qquad (A16)$$

The coefficient c_{Dia} handicaps diazotrophs by dampening the increase of their maximal growth rate vs. that of other phytoplankton with rising temperature. Diazotrophs can

The vicious N cycle

A. Landolfi

Full Screen / Esc

take up nitrate however, their growth rate is not limited by NO_3 concentrations:

$$\overline{J_{Dia}}(I, PO_4) = \min(J_{I/Dia}, J_{maxDia}u_{PO_4}), \tag{A17}$$

In addition to phosphate, diazotrophs can take up DOP as a P source when PO_4 concentrations are lower than $0.005 \, mmol \, P \, m^{-3}$

$$\overline{J_{Dia}}(I, DOP) = \min(J_{I/Dia}, J_{maxDia}u_{DOP}), \tag{A18}$$

where $u_{DOP} = DOP/(k_{DOP} + DOP)$ represents the DOP uptake rate. The low maximum growth rate relative to other phytoplankton, which mimics the high energy demand for fixing N_2, makes diazotrophs competitive in P replete regions only.

A3 Remineralization and denitrification

Particulate organic matter remineralizes to dissolved inorganic nutrients and dissolved organic matter at a constant remineralization rate μ_{D_N}. In oxic conditions the remineralization of particulate organic matter consumes oxygen assuming fixed elemental ratios $O_2 : N$, $N : P$ and $O_2 : P$ following Anderson 1995 (Table S.1) implicitly assuming instantaneous nitrification of NH_4 from organic matter remineralization. Oxygen consumption in suboxic waters ($< 5 \, \mu M$) is inhibited, according to

$$r_{sox}{}^{O_2} = 0.5(\tanh(O_2 - 5) + 1) \tag{A19}$$

and is replaced by the oxygen-equivalent of nitrate,

$$r_{sox}{}^{NO_3} = 0.5(1 - \tanh(O_2 - 5)). \tag{A20}$$

The on-set of canonical denitrification starts at $< 5 \, mmol \, m^{-3} \, O_2$ levels and proceeds until NO_3 is zero. There is no artificial NO_3 threshold as applied elsewhere[19]. As we have fixed stoichiometries[24] we implicitly assume complete denitrification (implicitly including the anammox reaction). Denitrification consumes nitrate at a rate of 80 % of the

molar oxygen equivalent rate, as NO_3^- is a more efficient oxidant on a mole per mole basis. Oxic and anoxic remineralization stop when both O_2 and NO_3 become zero. The model does not include sedimentary denitrification. Sinking detritus which accumulates at the ocean floor is remineralized following the same rules which hold everywhere else

5 in the water column.

A4   Grazing

Zooplankton grazing of Diazotrophs, $G(P_{Dia})$, and (non-nitrogen-fixing) phytoplankton $G(P)$ is parameterized using a sigmoidal function:

$$G(P_{Dia}) = \frac{g\epsilon P_{Dia}^2}{g + \epsilon P^2 + \epsilon P_{Dia}^2} \tag{A21}$$

10 $$G(P) = \frac{g\epsilon P^2}{g + \epsilon P_{Dia}^2 + \epsilon P^2} \tag{A22}$$

A5   Sinking of Detritus

The rate of sinking of Detritus w_s is a linear function of depth z but can not exceed a maximum value of w_{Dmax}:

15 $$w_s = w_s(z) = \min(w_{D0} + m_w z, w_{Dmax}). \tag{A23}$$

References

Altabet, M. A.: Constraints on oceanic N balance/imbalance from sedimentary 15N records, Biogeosciences, 4, 75–86, doi:10.5194/bg-4-75-2007, 2007. 8906, 8908

Altabet, M. A., Higginson, M. J., and Murray, D. W.: The effect of millennial-scale changes in Arabian Sea denitrification on atmospheric CO_2, Nature, 415, 159–162, 2002. 8906

Anderson, L.: On the hydrogen and oxygen content of marine phytoplankton. Deep-Sea Res. Pt. I, 42, 1675–1680, 1995. 8909, 8910, 8918

Bianchi, D., Dunne, J. P., Sarmiento, J. L. and Galbraith, E. D.: Data-based estimates of suboxia, denitrification, and N_2O production in the ocean and their sensitivities to dissolved O_2, Global Biogeochem. Cy., 26, GB2009, doi:10.1029/2011GB004209, 2012. 8928

Breitbarth, E., Oschlies, A., and LaRoche, J.: Physiological constraints on the global distribution of Trichodesmium – effect of temperature on diazotrophy, Biogeosciences, 4, 53–61, doi:10.5194/bg-4-53-2007, 2007. 8907, 8914

Canfield, D. E.: Models of oxic respiration, denitrification and sulfate reduction in zones of coastal upwelling, Geochim. Cosmochim. Ac., 70, 5753–5765, 2006. 8911

Capone, D. G., Zehr, J. P., Paerl, H. W., Bergman, B., and Carpenter, E. J.: Trichodesmium, a globally significant marine cyanobacterium, Science, 276, 1221–1229, 1997. 8907

Codispoti, L. A.: Phosphorus vs. nitrogen limitation of new and export production, in: Productivity of the Ocean: Present and Past, edited by: Berger, W. H., Smetacek, V. S. and Wefer, G., Wiley, New York, 377–394, 1989. 8907

Codispoti, L. A., Brandes, J. A., Christensen, J. P., Devol, A. H., Naqvi, S. W. A., Paerl, H. W., and Yoshinari, T.: The oceanic fixed nitrogen and nitrous oxide budgets: Moving targets as we enter the Anthropocene?, Sci. Mar., 65, 85–105, 2001. 8913, 8914

Conkright, M. E., et al.: World Ocean Atlas 2001: Objective Analyses, Data Statistics, and Figures, (CD-ROM Documentation), National Oceanographic Data Centre, Silver Spring, 1–17, 2002. 8908, 8909, 8911, 8930

Delaney, M. L.: Phosphorus accumulation in marine sediments and the oceanic phosphorus cycle, Global Biogeochem. Cy., 12, 563–572, 1998. 8907

Deutsch, C., Sarmiento, J. L., Sigman, D. M., Gruber, N., and Dunne, J. P.: Spatial coupling of nitrogen inputs and losses in the ocean, Nature, 445, 163–167, 2007. 8908, 8910, 8913, 8914

Discussion Paper | Discussion Paper | Discussion Paper | Discussion Paper | Discussion Paper

BGD

9, 8905–8930, 2012

The vicious N cycle

A. Landolfi

Title Page

Abstract | Introduction

Conclusions | References

Tables | Figures

◄ | ►

◄ | ►

Back | Close

Full Screen / Esc

Printer-friendly Version

Interactive Discussion

Devol, A. H.: Denitrification including anammox, in: Nitrogen in the Marine Environment 2nd Edition, edited by: Capone, D., Bronk, D., Mulholland, M., and Carpenter, E., Elsevier, Amsterdam, 263–301, 2008. 8907, 8909

Duce, R. A., LaRoche, J., Altieri, K., Arrigo, K. R., Baker, A. R., Capone, D. G., Cornell, S., Dentener, F., Galloway, J., Ganeshram, R. S., Geider, R. J., Jickells, T., Kuypers, M. M., Langlois, R., Liss, P. S., Liu, S. M., Middelburg, J. J., Moore, C. M., Nickovic, S., Oschlies, A., Pedersen, T., 5 Prospero, J., Schlitzer, R., Seitzinger, S., Sorensen, L. L., Uematsu, M., Ulloa, O., Voss, M., Ward, B., and Zamora, L.: Impacts of atmospheric anthropogenic nitrogen on the open ocean, Science, 320, 893–897, 2008. 8914

Falkowski, P. G.: Evolution of the nitrogen cycle and its influence on the biological sequestration of CO_2 in the ocean, Nature, 387, 272–275, 1997. 8906, 8907, 8914

Fernandez, C., Farías, L., and Ulloa, O.: Nitrogen fixation in denitrified marine waters, PLoS One, 6, 20539, 2011. 8908, 8914

Gnanadesikan, A. et al.: GFDL's CM2 Global Coupled Climate Models, Part II: The Baseline Ocean Simulation, J. Climate, 19, 675–697, 2005. 8908

Gruber, N.: The dynamics of the marine nitrogen cycle and its influence on atmospheric CO_2. in: Carbon Climate Interactions, edited by: Oguz, T. and Follows, M., Kluwer, Dordrecht, 97–148, 2004. 8906, 8907, 8908

Large, W. and Yeager, S.: Diurnal to decadal global forcing for ocean and sea-ice models: the data sets and flux climatologies, CGD Division of the National Center for Atmospheric Research, 105 pp., 2004. 8908

Laws E. A.: Photosynthetic quotients, new production and net community production in the open ocean, Deep-Sea Res. Pt. I, 38, 143–167, 1991. 8911

Lenton, T. M. and Watson, A. J.: Redfield revisited 1. Regulation of nitrate, phosphate, and oxygen in the ocean, Global Biogeochem. Cy., 14, 225–248, 2000. 8907

Mahowald, N. M., Muhs, D. R., Levis, S., Rasch, P. J, Yoshioka, Zender, C. S., and Luo C.: Change in atmospheric mineral aerosols in response to climate: Last glacial period, preindustrial, modern, and doubled carbon dioxide climates, J. Geophys. Res., 111, D10202, doi:10.1029/2005JD006653, 2006. 8914

Martin, J. H., Knauer, G. A., Karl, D. M., and Broenkow, W. W.: VERTEX: carbon cycling in the Northeast Pacific, Deep-Sea Res., 34, 267–285, 1987. 8928

Mills, M. M. and Arrigo, K.: Magnitude of oceanic nitrogen fixation influenced by the nutrient uptake ratio of phytoplankton, Nature, 3, 412–416, 2010. 8907

The vicious N cycle

A. Landolfi

Moisander, P. et al.: Unicellular cyanobacterial distributions broaden the oceanic N_2 fixation domain, Science, 327, 1512–1514, 2008. 8914

Moore, J. K. and Doney, S. C.: Iron availability limits the ocean nitrogen inventory stabilizing feedbacks between marine denitrification and nitrogen fixation, Global Biogeochem. Cy., 21, GB2011, doi:10.1029/2006GB002762, 2007. 8907, 8910, 8913

Moore, C. M., Mills, M. M., Achterberg, E. P., Geider, R. J., LaRoche, J., Lucas, M. I., McDonagh, E. L., Pan, X., Poulton, M., Rijkenberg, J. A., Suggett, D. J., Ussher S. J., and Woodward, E. M. S.: Large-scale distribution of Atlantic nitrogen fixation controlled by iron availability, Nature, 2, 867–871, doi:10.1038/ngeo667, 2009. 8907

Paulmier, A., Kriest, I., and Oschlies, A.: Stoichiometries of remineralisation and denitrification in global biogeochemical ocean models, Biogeosciences, 6, 923–935, doi:10.5194/bg-6-923-2009, 2009. 8910

Redfield, A. C., Ketchum, B. .H., and Richards F. A.: The influence of organisms on the composition of sea water, in: The Sea Vol. 2, edited by: Hill, M. N., Wiley-Interscience, New York, 26–77, 1963. 8907

Schmittner, A., Oschlies A., Matthews H. D., and Galbraith E. D.: Future changes in climate, ocean circulation, ecosystems and biogeochemical cycling simulated for a business-as-usual CO_2 emission scenario until 4000 AD, Global Biogeochem. Cy., 22, GB1013, doi:10.1029/2007GB002953, 2008. 8908, 8910, 8913

Stramma, L., Johnson, G. C., Sprintall, J., and Mohrholz, V.: Expanding oxygen-minimum zones in the tropical oceans, Science, 320, 655–658, 2008. 8914

Tyrrell, T.: The relative influences of nitrogen and phosphorus on oceanic primary production, Nature, 400, 525–531, 1999. 8907

Title Page

Abstract | Introduction

Conclusions | References

Tables | Figures

◀ | ▶

◀ | ▶

Back | Close

Full Screen / Esc

Printer-friendly Version

Interactive Discussion

Table A1. Ocean ecosystem model parameters.

| Ecosystem model parameter	Symbol	Value	Unit
Phytoplankton (P) Coefficients			
Initial slope of P–I curve	α	0.025	$day^{-1}/(W\,m^{-2})$
Maximum growth rate	a	0.6	day^{-1}
E-folding temperature of biotic rates	T_b	15.65	$°C$
Half-saturation constant for NO_3 uptake	k_{NO_3}	0.5	$mmol\,m^{-3}$
Half-saturation constant for PO_4 uptake	k_{PO_4}	0.3	$mmol\,m^{-3}$
Half-saturation constant for DOP uptake	k_{DOP}	0.3	$mmol\,m^{-3}$
Specific mortality rate of phytoplankton	μ_P	0.03	day^{-1}
Diazotroph (P_{Dia}) Coefficients			
Dampening of maximal growth rate	c_{Dia}	0.5	
Specific mortality rate of diazotrophs	μ_{Dia}	0.02	day^{-1}
Zooplankton (Z) Coefficients			
Assimilation efficiency	γ_1	0.75	
Maximum grazing rate	g	2.0	day^{-1}
Prey capture rate	ϵ	1.0	$(mmol\,m^{-3})^{-2}\,day^{-1}$
(Quadratic) mortality	μ_Z	0.2	$(mmol\,m^{-3})^{-2}\,day^{-1}$
Excretion	γ_2	0.03	day^{-1}
DOM Coefficients			
Fraction of phy. mortality into DOM	σ_{P_m}	0.5	
Fraction of dia. mortality into DOM	σ_{Dia_m}	0.5	
Fraction of zoo. sloppy feeding into DOM	σ_{Z_s}	0.5	
Fraction of zoo. excretion into DOM	σ_{Z_e}	0.5	
Fraction of zoo. mortality into DOM	σ_{Z_m}	0.05	
Fraction of det. N into DON	σ_{D_N}	0.1	
Fraction of det. P into DOP	σ_{D_P}	0.1	
DON remin. rate	μ_{DON}	0.01	day^{-1}
DOP remin. rate	μ_{DOP}	0.01	day^{-1}
Detrital (D) Coefficients			
Detrital N remineralization rate	μ_{D_N}	0.05	day^{-1}
Sinking speed at surface	w_{D0}	7	$m\,day^{-1}$
Increase of sinking speed with depth	m_w	0.04	day^{-1}
Maximum sinking speed in water column	w_{Dmax}	40	$m\,day^{-1}$
Detrital P remineralization rate	μ_{D_P}	0.05	day^{-1}
Molar elemental ratios			
Elemental O_2 : P	R_O	150	
Phytoplakton elemental N : P	R	16	
Diazotroph elemental N : P	R_{Dia}	16	
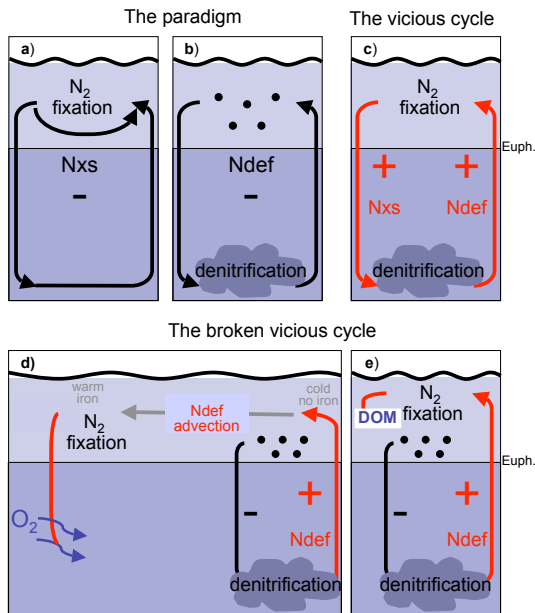
Fig. 1. Feedbacks of the marine nitrogen cycle. Negative feedbacks (black) reduce the initial perturbation. Positive feedbacks (red) amplify the initial perturbation. Negative feedback ensue when the two process occur individually: **(a)** N_2 fixation is self-limited via production of excess nitrogen (Nxs), and **(b)** denitrification, is self-limited by the generation of nitrogen deficits (Ndef) that reduce non-fixing phytoplankton export production. Spatially coupled denitrification and N_2 fixation give rise to a vicious cycle consisting of a positive feedback between the two processes **(c)**. To break the vicious cycle and allow for the self-limiting individual processes of panels **(a)** and **(b)** to dominate, a spatial decoupling of areas of N_2 fixation and denitrification can either occur laterally **(d)** or vertically **(e)** mediated by effects of temperature, iron or dissolved organic matter and oxygen injections. Light shading represents the euphotic zone and dark shading the low-oxygen waters where denitrification can take place. Black dots represent "non-fixing" phytoplankton. Positive and negative signs and red and black arrows represent positive and negative feedback, respectively.

The vicious N cycle

A. Landolfi

Title Page

Abstract	Introduction
Conclusions	References
Tables	Figures

|◄   ►|

◄   ►

Back   Close

Full Screen / Esc
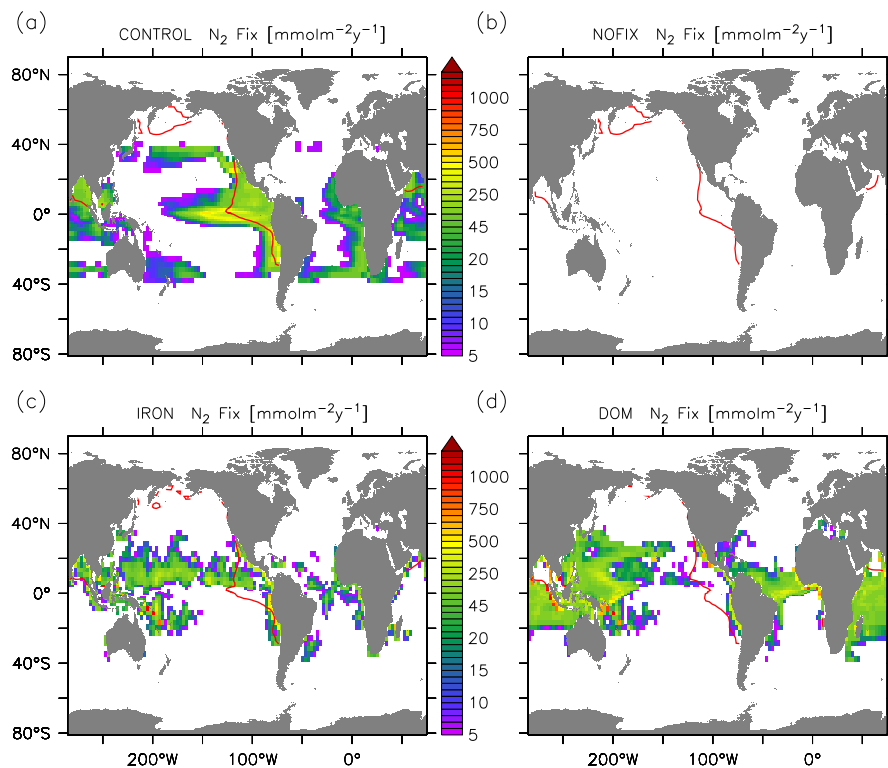
Fig. 2. 150-yr mean N2 fixation rates ($mmol\,N\,m^{-2}\,y^{-1}$) calculated for the **(a)** CONTROL, **(b)** NOFIX, **(c)** IRON and **(d)** DOM simulation. Red contour denotes the average position of the $5\,mmol\,m^{-3}$ O_2 isoline of the vertical minimum of dissolved oxygen.
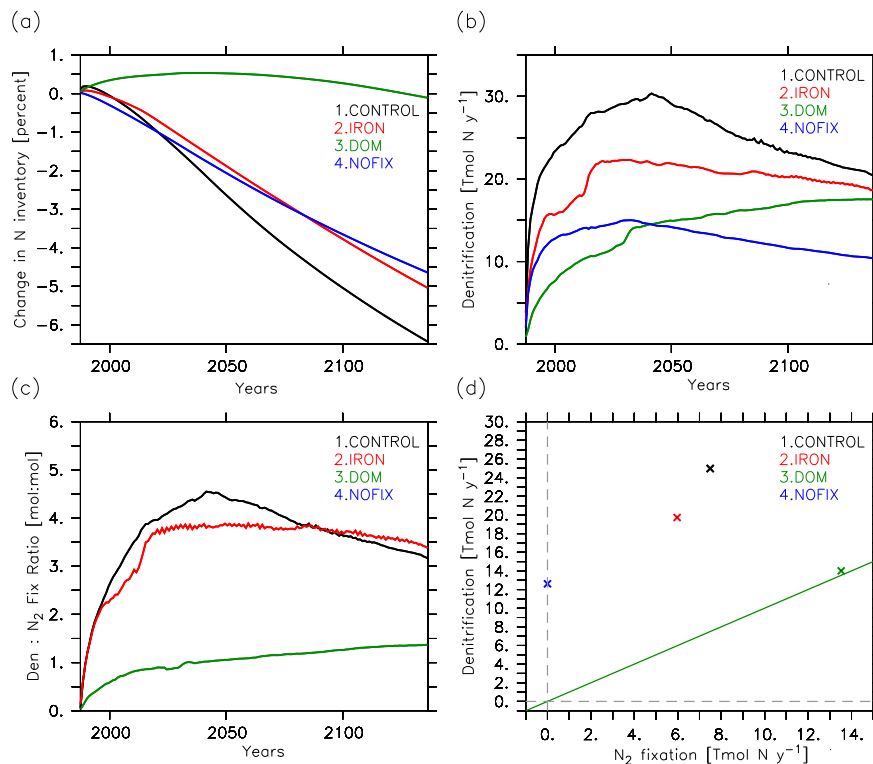
Fig. 3. Temporal evolution of **(a)** oceanic N inventory (changes in %), **(b)** global denitrification rates (TmolN yr^{-1}), **(c)** ratio of global denitrification to global N$_2$ fixation (mol : mol). Panel **(d)** shows scatter plots of the 150-yr mean global denitrification versus 150-yr mean global N$_2$ fixation for the CONTROL, NOFIX, IRON and DOM and simulations. The green line has slope 1and indicates a balanced oceanic nitrogen inventory.

Title Page

Abstract | Introduction

Conclusions | References

Tables | Figures

|◄ | ►|

◄ | ►

Back | Close

Full Screen / Esc

Printer-friendly Version

Interactive Discussion
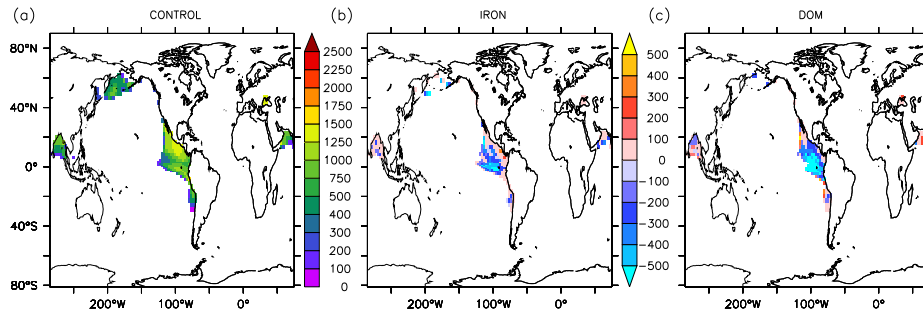
Fig. 4. Average thickness (m) of the low O_2 water layer (lower than $5\,\mathrm{mmol\,m^{-3}}$) in the CONTROL simulation (panel **a**). Panel **(b)** and **(c)** are thickness changes of the **(b)** IRON and **(c)** DOM simulations relative to the CONTROL simulation. Thickness changes are in units (m) with negative numbers denoting reductions relative to the CONTROL simulation.
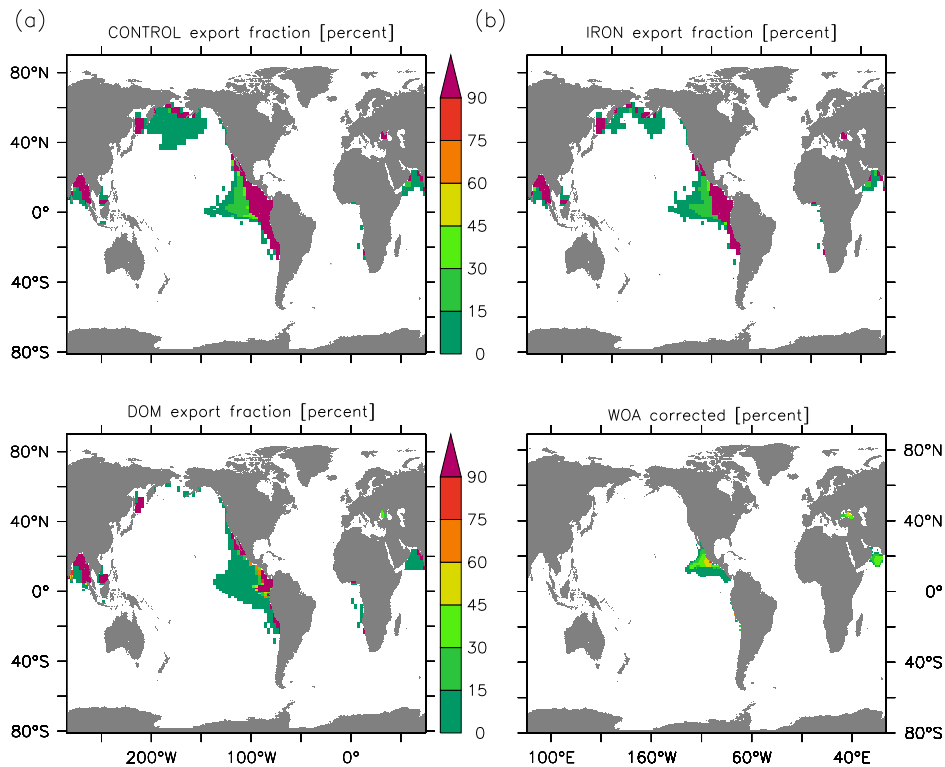
Fig. 5. 150-yr mean fraction of export remineralized in OMZ zones (O_2 lower than $5\,\mathrm{mmol\,m^{-3}}$) for the **(a)** CONTROL, **(b)** IRON and **(c)** DOM simulations, and (d) fraction of export remineralized in OMZ according to a combination of the Martin curve (Martin et al., 1987) and the corrected WOA annual mean O_2 concentrations (Bianchi et al., 2012). The onset of a vicious cycle occurs in regions where >15 % of the export is remineralized in suboxic waters.
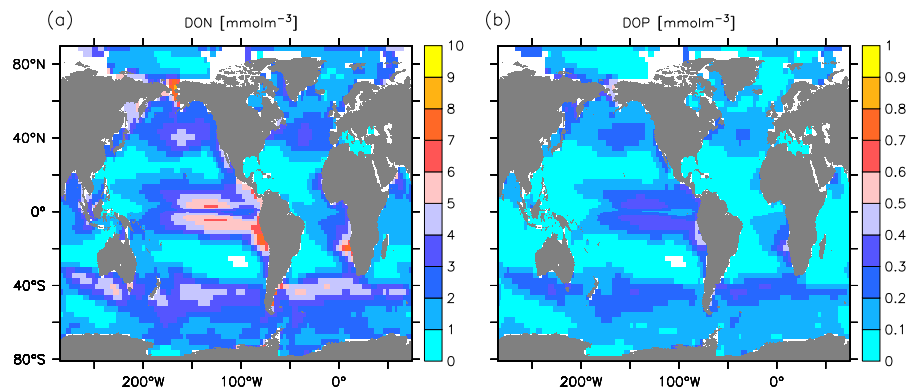
Fig. 6. 150-yr mean **(a)** DON and **(b)** DOP upper ocean (0–100 m) concentrations of the DOM simulation.
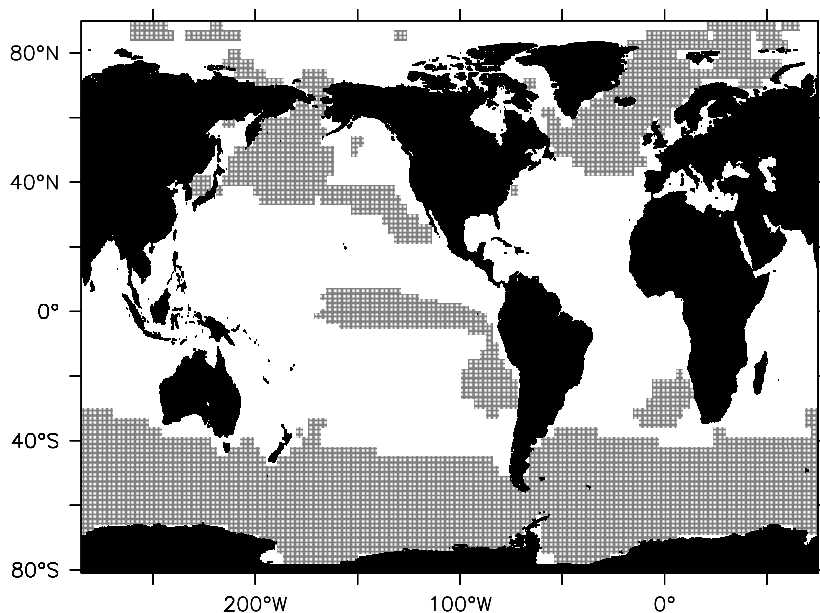
Fig. A1. Diagnosed iron mask, 150 yr average. Shading denotes areas where phytoplankton growth rates in the IRON and DOM simulations are reduced locally such that, simulated surface PO_4 concentrations do not exceed observed PO_4 monthly mean concentrations from the World Ocean Atlas (WOA) (Conkright et al., 2002).